Fluids 6, 1169 (1963).
[9]B. Coppi, J. M. Greene, and J. L. Johnson, Nucl. Fusion 6, 101 (1966).
[10]B. Coppi, G. Laval, and R. Pellat, Phys. Rev. Letters 16, 1207 (1966).
[11]E. M. Barston, Phys. Fluids 12, 2162 (1969).
[12]A. D. Jette, J. Math. Anal. Appl. 29, 109 (1970).
[13]B. Coppi, in *Propagation and Instabilities in Plasmas*, edited by W. I. Futterman (Stanford U. P., Stanford, Calif., 1963).
[14]P. H. Rebut, J. Nucl. Energy 4, 159 (1962).

PHYSICAL REVIEW A VOLUME 4, NUMBER 4 OCTOBER 1971

Multiple Scattering of Neutrons in Gaseous and Liquid Methane*

Ashok K. Agrawal
Reactor Analysis and Safety Division, Argonne National Laboratory, Argonne, Illinois 60439
(Received 7 May 1971)

A "factor method" of evaluating the double-scattering correction for inelastic-neutron-scattering experiments with an infinite-plane-slab specimen has been developed. Using appropriate dynamical models, calculations have been made both for highly compressed room-temperature gaseous methane and for liquid methane at 98°K. As a result, the agreement between analytical results with measurements is remarkably improved. In addition, the model sensitivity of the correction and the advantages of reflection-type experimental geometry over transmission-type are investigated.

I. INTRODUCTION

The use of slow neutrons as a probe to investigate molecular dynamics is considered to be a very powerful technique. The experimentally observed scattered-neutron intensities are usually interpreted with a phenomenological molecular-dynamics model. The success of such an interpretation depends on measuring single-scattering intensity for a monoenergetic incident neutron beam and an infinite-resolution detector. Such idealized experimental requirements are never achieved; hence, analytical results should include the effects of second- and higher-order scatterings and of the finite resolution of the incident beam and the detector. Of these three factors, multiple scattering appears to be the most complicated one to account for. The problems mentioned here are not peculiar to inelastic-neutron-scattering experiments, but rather are common to a wide variety of different experiments. We will confine ourselves only to inelastic-neutron-scattering experiments.

A workable scheme for evaluating the multiple-scattering correction was first given by Vineyard,[1] who solved an energy-independent neutron-transport equation for an infinite-plane-slab specimen. Subsequently, Blech and Averbach[2] have extended the method to infinite cylindrical samples. Both of these investigations were restricted to elastic scattering of neutrons under the assumption of a quasi-isotropic scattering cross section. Cocking and Heard[3] have calculated second-order scattering without making use of the quasi-isotropic approximation.

Recently, the effects of second-order scattering have been studied by Slaggie,[4] as well as by others,[5] who solved the energy-dependent neutron-transport equation for transmission-type experiments. A common conclusion of these workers is that the second-order scattering correction is very important and quite sensitive to the details of the scattering cross section.

In this paper we describe in Sec. II a "factor method" of evaluating second-order corrections for both transmission- and reflection-type experimental geometries. Resulting expressions are then programmed[6] to evaluate the correction for an arbitrary scattering law. In Sec. III numerical results are obtained for three different geometrical sample thicknesses for room-temperature gaseous methane with a liquid density. These results are directly applicable to Larsson's experiment.[7] Section III also deals with a comparison of our results with cold-neutron liquid-methane data of Dasannacharya and Venkataraman.[8] The finite resolution of the incident neutron beam is accounted for in a suggested approximate manner. Scattering-law model sensitivity and advantages of reflection geometry over transmission geometry are discussed along with some concluding remarks in Sec. IV.

II. THEORY

We consider a scattering sample in which the scatterers may or may not be uniformly distributed. We assume that a monoenergetic neutron beam of energy E_0 is incident at a direction defined by the vector $\vec{s}_0$. The nth-order scattered-neutron density is then the solution of the following transport equation[1]:

$$\vec{s}\cdot\vec{\nabla}P_n(E,\vec{r},\vec{s})+\Sigma(E)P_n(E,\vec{r},\vec{s}) = \int\int dE'd\Omega'\,\sigma(E'\to E,\vec{s}'\to\vec{s})P_{n-1}(E',\vec{r},\vec{s}'),\quad n=0,1,2,\ldots \tag{1}$$

where $P_{-1}\equiv 0$, $P_n(E,\vec{r},\vec{s})$ is the number of nth-order scattered neutrons per unit volume of energy E within unit energy increment, which are proceeding in the direction $\vec{s}$; $\Sigma(E)$ is the macroscopic total cross section at energy E; and $\sigma(E'\to E,\vec{s}'\to\vec{s})$ is the double-differential macroscopic cross section for scattering from energy E' to E and direction $\vec{s}'$ to $\vec{s}$. The formal solution of Eq. (1) may be written as

$$P_0(E,\vec{r},\vec{s}) = P_0(E,\vec{r}-L\vec{s},\vec{s})\delta(E-E_0)\times\delta(\vec{s}-\vec{s}_0)\,e^{-\Sigma(E_0)L} \tag{2}$$

and

$$P_n(E,\vec{r},\vec{s}) = \int\int dE'd\Omega'\,\sigma(E'\to E,\vec{s}'\to\vec{s})\times\int_0^L d\xi\, e^{-\Sigma(E)\xi}P_{n-1}(E',\vec{r}-\xi\vec{s},\vec{s}'),\quad n=1,2,\ldots \tag{3}$$

where L is the chord length from the point $\vec{r}$ to the surface of the sample in the direction $-\vec{s}$, as shown in Fig. 1. It is assumed that the sample is nowhere concave. The problem of calculating higher-order scattering intensities is in principle solved by an iterative procedure by combining Eqs. (2) and (3). Since the integrals involved are generally difficult to evaluate, we restrict ourselves to the infinite plane-slab geometry. In this case, the expressions for P_0 and P_n become

$$P_0(E,z,\vec{s}) = (1/2\pi)\,e^{-\Sigma(E)L}\delta(\cos\theta-\cos\theta_0)\delta(E-E_0) \tag{4}$$

and

$$P_n(E,z,\vec{s}) = \int\int dE'd\Omega'\,\sigma(E'\to E,\vec{s}'\to\vec{s})\times\int_0^L d\xi\, e^{-\Sigma(E)\xi}P_{n-1}(E',z-\xi\cos\theta,\vec{s}'),\quad n=1,2,\ldots \tag{5}$$

where the system of coordinates chosen to describe the vector $\vec{s}$ is shown in Fig. 2. The chord length L is related to the slab thickness t

$$L = z\sec\theta \quad \text{if } \theta<\tfrac{1}{2}\pi$$
$$= (z-t)\sec\theta \quad \text{if } \theta>\tfrac{1}{2}\pi\,. \tag{6}$$

Expressions for the first- and higher-order scattered-neutron intensities can now be obtained by iterating Eqs. (4) and (5). We note down the general results for P_1 and P_2:

$$P_1(E,z,\vec{s}) = \sigma(E_0\to E,\vec{s}_0\to\vec{s})\sec\theta\times\frac{e^{-\Sigma_0 z\sec\theta_0}-h(\theta)e^{-\Sigma z\sec\theta}}{\Sigma\sec\theta-\Sigma_0\sec\theta_0} \tag{7}$$

and

$$P_2(E,z,\vec{s}) = \int\int dE'd\Omega'\,\sigma(E'\to E,\vec{s}'\to\vec{s})\times\sigma(E_0\to E',\vec{s}_0\to\vec{s}')G(\theta,\theta'), \tag{8}$$

where

$$h(\theta)=1 \quad \text{if } \theta<\tfrac{1}{2}\pi$$
$$= e^{\Sigma t\sec\theta-\Sigma_0 t\sec\theta_0} \quad \text{if } \theta\geq\tfrac{1}{2}\pi\,, \tag{9}$$

$$G(\theta,\theta') = \frac{\sec\theta\sec\theta'}{\Sigma'\sec\theta'-\Sigma_0\sec\theta_0}\left(\frac{e^{-\Sigma_0 z\sec\theta_0}-h(\theta)e^{-\Sigma z\sec\theta}}{\Sigma\sec\theta-\Sigma_0\sec\theta_0} - \frac{e^{-\Sigma' z\sec\theta'}-h(\theta)e^{-\Sigma z\sec\theta}}{\Sigma\sec\theta-\Sigma'\sec\theta'}\,h(\theta')\right); \tag{10}$$

$\Sigma\equiv\Sigma(E)$, and $h(\theta')$ is defined by Eq. (9) when Σ and θ are replaced by their corresponding primed quantities. Higher-order corrections, which are small, involve extremely complicated expressions and hence are not attempted. The current of nth-order scattered neutrons J_n which leave the surface of the slab is obtained by multiplying P_n by the normal component of the velocity.

Thus, we obtain

$$J_n(E,z,\vec{s}) = \left(\frac{E}{E_0}\right)^{1/2}\frac{\cos\theta}{\cos\theta_0}P_n(E,z,\vec{s})\,. \tag{11}$$

The double-scattering correction can now be estimated by evaluating the first- and second-order scattered neutron currents. The above expressions can further be simplified for a specimen in which the scatterers are randomly distributed; i.e., for a given neutron energy the scattering cross section depends only on the angle of scattering. For these cases, Eq. (8) becomes

$$P_2(E,z,\vec{s}) = \int\int dE'd\Omega'\,\sigma(E'\to E,\vec{s}'\cdot\vec{s})$$

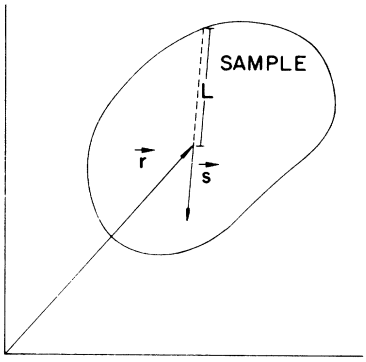

FIG. 1. Geometry of the general case.

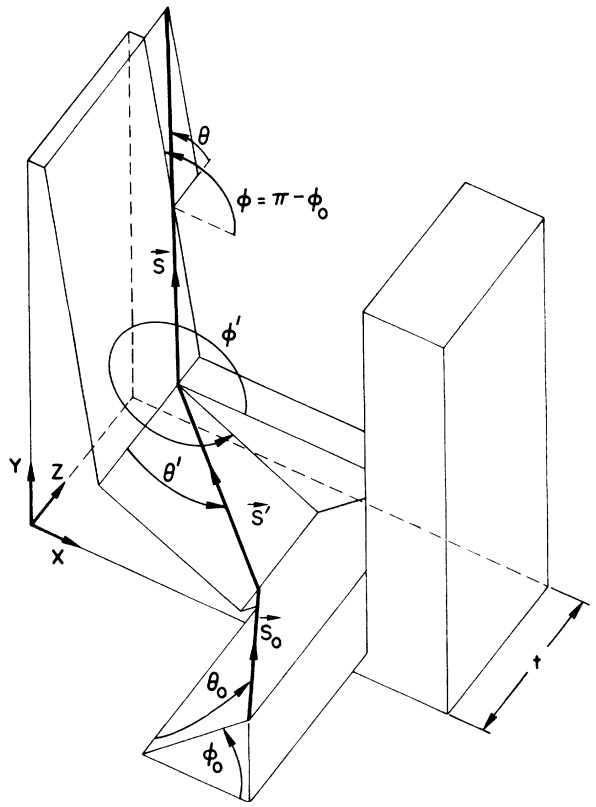

FIG. 2. Geometry of the plane slab.

$$\times \sigma(E_0 \to E', \vec{s}_0 \cdot \vec{s}')G(\theta, \theta') , \qquad (12)$$

where the cosines of the first and second scattering angles are given by

$$\cos(\vec{s}_0 \cdot \vec{s}') = \cos\theta_0 \cos\theta' + \sin\theta_0 \sin\theta' \cos(\phi' - \phi_0) \qquad (13)$$

and

$$\cos(\vec{s}' \cdot \vec{s}) = \cos\theta' \cos\theta + \sin\theta' \sin\theta \cos(\phi - \phi') . \qquad (14)$$

Vectors $\vec{s}_0$, and $\vec{s}$ and the normal to the sample are usually coplanar. In this case, we have $\phi = \pi - \phi_0$. Furthermore, we can choose our coordinate system in such a way that $\phi_0 = 0$. Equations (13) and (14) then become

$$\cos(\vec{s}_0 \cdot \vec{s}') = \cos\theta_0 \cos\theta' + \sin\theta_0 \sin\theta' \cos\phi' \qquad (15)$$

and

$$\cos(\vec{s}' \cdot \vec{s}) = \cos\theta' \cos\theta - \sin\theta' \sin\theta \cos\phi' . \qquad (16)$$

The first- and second-order scattered neutron currents can now be calculated by combining Eqs. (7), (11), and (12). Note that the calculation of J_1 is straightforward, since it is related to the double-differential scattering cross section through a "geometric factor," while a triple integration over variables E', and θ', and ϕ' needs to be performed numerically for J_2. The expression for J_2 can be written in a simpler form by expressing the double-differential cross section in forms of the "scattering law" $S(\kappa, \omega)$ of the scatterer:

$$\sigma(E_0 \to E, \alpha) = (\sigma_0/4\pi)(E/E_0)^{1/2} S(\kappa, \omega) , \qquad (17)$$

where momentum- and energy-transfer variables are given by[9]

$$\kappa = (2m)^{1/2}[E + E_0 - 2(EE_0)^{1/2}\cos\alpha]^{1/2} ,$$
$$\omega = (E - E_0) , \qquad (18)$$

σ_0 is the bound-atom macroscopic scattering cross section, m is the neutron mass, and α is the angle of scattering. By combining Eqs. (7), (11), (12), and (17) and rearranging, we get

$$J_1(E, z, \vec{s}) = (E/E_0)(\sigma_0/4\pi) S(\kappa, \omega) f(\theta) , \qquad (19)$$

$$J_2(E, z, \vec{s}) = (E/E_0)(\sigma_0^2/8\pi) \int dE' \int_0^{\pi} \sin\theta' \, d\theta' \times I(\theta') F(\theta, \theta') , \qquad (20)$$

where

$$f(\theta) = \sec\theta_0 \frac{e^{-\Sigma_0 z \sec\theta_0} - h(\theta) e^{-\Sigma z \sec\theta}}{\Sigma \sec\theta - \Sigma_0 \sec\theta_0} , \qquad (21)$$

$$I(\theta') = (1/2\pi) \int_0^{2\pi} S(\kappa_2, \omega_2) S(\kappa_1, \omega_1) \, d\phi' , \qquad (22)$$

$$F(\theta, \theta') = \sec\theta_0 G(\theta, \theta') , \qquad (23)$$

and $\kappa_1(\omega_1)$ and $\kappa_2(\omega_2)$ are, respectively, the momentum-transfer (energy-transfer) variables for first- and second-order scattering, defined by equations similar to Eq. (18). Several special cases of interest are now considered.

A. Elastic Scattering

Change of neutron energy due to a scattering collision with the scatterer is not considered. By dropping the energy variable from the J_n's and Σ's in Eqs. (19)–(22), we obtain the following expressions for the first- and second-order scattered-neutron currents:

$$J_1(z, \vec{s}) = \frac{\sigma_0}{4\pi\Sigma} S(\kappa, 0) \frac{e^{-\Sigma z \sec\theta_0} - h(\theta) e^{-\Sigma z \sec\theta}}{\sec\theta \cos\theta_0 - 1} \qquad (24)$$

and

$$J_2(z, \vec{s}) = (\sigma_0^2/8\pi) \int_0^{\pi} \sin\theta' d\theta' I_e(\theta') F(\theta, \theta') , \qquad (25)$$

where

$$I_e(\theta') = (1/2\pi) \int_0^{2\pi} S(\kappa_2, 0) S(\kappa_1, 0) \, d\phi' . \qquad (26)$$

As a special case, for transmission experiments, the above results reduce to those obtained by Vineyard.[1] The quasistatic approximation of Vineyard can be obtained by setting $I_e(\theta') = 1$.

B. Transmission Experiment

We now consider the problem of calculating the first- and second-order scattered currents for inelastic-neutron-scattering experiments in which the detector is placed on the opposite side of the incident beam. In this case the angle between the detector and slab normal is always less than 90°. The desired expressions for J_1 and J_2 are obtained by substituting $z = t$ (slab thickness) in Eqs. (19)–(21). Results are given by Eqs. (19) and (20), provided that the $f(\theta)$ occurring in Eq. (19) is replaced by $f_t(\theta)$ and the $F(\theta, \theta')$ appearing in Eq. (20) is replaced by $F_t(\theta, \theta')$:

$$f_t(\theta) = \sec\theta_0 \frac{e^{-\Sigma_0 t \sec\theta_0} - e^{-\Sigma t \sec\theta}}{\Sigma \sec\theta - \Sigma_0 \sec\theta_0} , \tag{27}$$

$$F_t(\theta, \theta') = \frac{\sec\theta_0 \sec\theta'}{\Sigma' \sec\theta' - \Sigma_0 \sec\theta_0} \left(\frac{e^{-\Sigma_0 t \sec\theta_0} - e^{-\Sigma t \sec\theta}}{\Sigma \sec\theta - \Sigma_0 \sec\theta_0} - \frac{e^{-\Sigma' t \sec\theta'} - e^{-\Sigma t \sec\theta}}{\Sigma \sec\theta - \Sigma' \sec\theta'} h(\theta') \right) . \tag{28}$$

The scattering angle is $|\theta - \theta_0|$.

C. Reflection Experiment

In a reflection-type experiment, the detector is placed on the same side of the scattering slab as the incident beam. In our notation, the angle which the scattered beam makes with the slab normal is therefore always greater than 90°. Expressions for J_1 and J_2 can similarly be obtained by setting $z = 0$ in Eqs. (19)–(21). Results are once again given by Eqs. (19) and (20), provided that the $f(\theta)$ and $F(\theta, \theta')$, occurring in these equations are replaced by $f_r(\theta)$ and $F_r(\theta, \theta')$, respectively. These functions are related to their counterparts for transmission experiments by the following equations:

$$f_r(\theta) = -e^{\Sigma t \sec\theta} f_t(\theta) \tag{29}$$

and

$$F_r(\theta, \theta') = -e^{\Sigma t \sec\theta} F_t(\theta, \theta') . \tag{30}$$

Minus signs appearing in these equations indicate that the first- and second-order scattered-neutron currents would have a negative sign, which is in agreement with our convention. The scattering angle is again $|\theta - \theta_0|$.

III. RESULTS

The above expressions [i.e., Eqs. (24)–(30)] for the first- and second-order scattered currents have been programmed in the DBLSCAT code[6] for both transmission- and reflection-type experiments. The code evaluates the second-order scattering correction for an arbitrary scattering law. In cold-neutron experiments, one usually measures scattered-neutron intensities in the time-of-flight scale. Hence, for direct comparison, the above results are transformed to the time-of-flight scale by the following relation:

$$J(\tau, t, \vec{s}) = 2(2/m)^{1/2} E^{3/2} J(E, t, \vec{s}) , \tag{31}$$

where τ is the time of flight of the scattered neutron.

We have obtained numerical results for the double-scattering correction for both gaseous- and liquid-methane slow-neutron scattering experiments. In the case of the room-temperature gaseous-methane experiment of Larsson,[7] calculations have been made at a pressure of 1500 atm for a sample density of 0.466 g/cm^3, which is the liquid-methane density at 109 °K. Since the free-molecule description for both translational and rotational motions is not expected to be valid under these conditions, we have used a Langevin-diffusion-type molecular-dynamics model. In the Gaussian approximation, the scattering law $S(\kappa, \omega)$ is given by[10]

$$S(\kappa, \omega) = e^{-\omega/2T} e^{-(\kappa^2/8MT)G(T)} (1/\pi) \int_0^\infty dt \cos\omega t \times e^{-(\kappa^2/2)W(t)} , \tag{32}$$

where the total width function $W(t)$ is approximated by a sum of its translational and rotational contributions:

$$W(t) = W_t(t) + W_r(t) , \tag{33}$$

$$W_t(t) = (2T/M\eta^2)(\eta t - 1 + e^{-\eta t}), \tag{34}$$

$$W_r(t) = \tfrac{2}{3} b^2 [1 - F_1(t)] , \tag{35}$$

and

$$F_1(t) = \exp[-(2T/I\xi^2)(\xi t - 1 + e^{-\xi t})] . \tag{36}$$

In these equations η and ξ are, respectively, the translational and rotational diffusion parameters, M is the molecular mass, I is the moment of inertia, b is the interatomic distance between C and H, and $G(T)$ is defined in Ref. 10 and for methane is roughly equal to 5.0. Note that our current choice of model ensures correct short- and long-time behaviors for both molecular translational and intramolecular rotational motions. Parameters η and ξ are related to their corresponding diffusion coefficients:

$$\eta = T/MD , \quad \xi = T/ID_r . \tag{37}$$

In the present computations we have used the experimental value of η (5.63×10^{12} sec^{-1}), and ξ is derived by assuming the dimensionless quantity $(T/I)^{1/2} \xi$ to be 0.5. This dimensionless value was found to give satisfactory agreement[10] with the first-order correlation function inferred from the infrared data for liquid methane at 98 °K.

Results of our estimates of the double-scattering correction are shown in Figs. 3 and 4. In these figures we have plotted the ratio of $(J_1 + J_2)/J_1$ as a function of the parameter of interest for a highly-

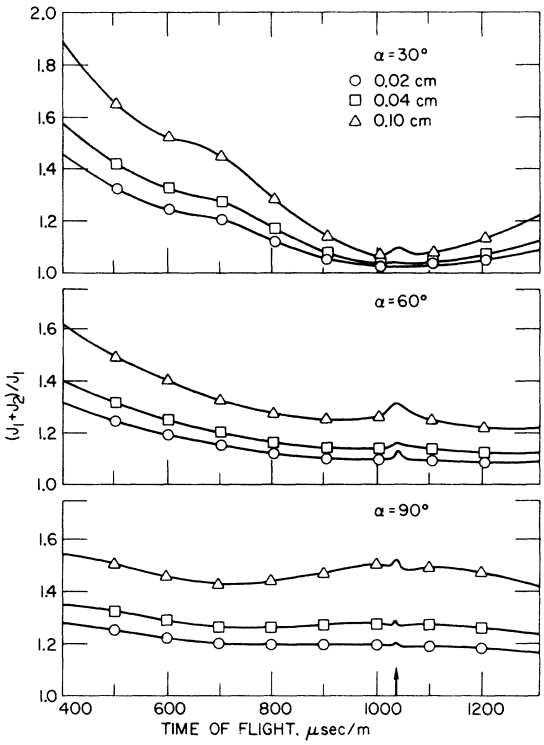

FIG. 3. $(J_1+J_2)/J_1$ vs time of flight in gaseous methane ($\Sigma = 4.56$ cm^{-1}) for different sample thicknesses and scattering angles. Incident neutron energy is shown by the arrow.

compressed room-temperature gaseous-methane in a transmission geometry for three different slab thicknesses (0.02, 0.04, and 0.10 cm). Using the macroscopic total cross section $\Sigma_0 = 4.56$ cm^{-1} at the incident neutron energy (4.87 meV), slab thicknesses correspond to transmission factors of 0.913, 0.833, and 0.634. Note that the double-scattering corrections are extremely important in inelastic region for small scattering angles. However, the correction depends only slightly on scattered-neutron energy for a scattering angle of 90°. The peak at the incident neutron energy is due to a predominant quasi-elastic peak in the scattering law. Figure 4 shows the extent of the double-scattering correction as a function of the sample thickness for different scattering angles and two neutron energies. The correction is seen to be significant even for a very thin sample. As a rule, the double-scattering correction is more important in the inelastic region than in the elastic region.

For a direct comparison of once- and twice-scattered-neutron intensities with measurements, analytical results must include the effect of finite resolution of the incident neutron beam and the detector response. In other words, the measured scattering intensities should be compared with the calculated one, which is given by

$$\sigma(\tau_0, \tau, \alpha) = \int\int \sigma'(\tau_0, \tau, \alpha) f(\tau_0)\, d\tau_0 R(\tau)\, d\tau \ , \quad (38)$$

where

$$\sigma'(\tau_0, \tau, \alpha) = \sigma_1(\tau_0, \tau, \alpha)\left(1 + \frac{\sum_{n=2}^{\infty} J_n(\tau, t, \alpha)}{J_1(\tau, t, \alpha)}\right) \ , \quad (39)$$

$\sigma_1(\tau_0, \tau, \alpha)$ is the double-differential scattering cross section for a single scattering event, and $f(\tau_0)$ and $R(\tau)$ are, respectively, the unit-normalized incident neutron beam spectrum and the detector response function. The quantity in parentheses in Eq. (39) is the multiple-scattering correction. Exact evaluation of $\sigma(\tau_0, \tau, \alpha)$, as given by Eq. (38), is extremely time consuming. Hence, approximate results are obtained by combining Eqs. (38) and (39), and then taking the multiple-scattering correction term out of the integration.[11] We get

$$\sigma(\tau_0, \tau, \alpha) \approx \left[\int\int \sigma_1(\tau_0, \tau, \alpha) f(\tau_0) d\tau_0 R(\tau)\, d\tau\right] \times \left(1 + \frac{\sum_{n=2}^{\infty} J_n(\tau, t, \alpha)}{J_1(\tau, t, \alpha)}\right) \ . \quad (40)$$

If only second-order scattering corrections are considered, then the summation in the above equation is replaced by the $n = 2$ term only.

Figure 5 shows a comparison of our results in

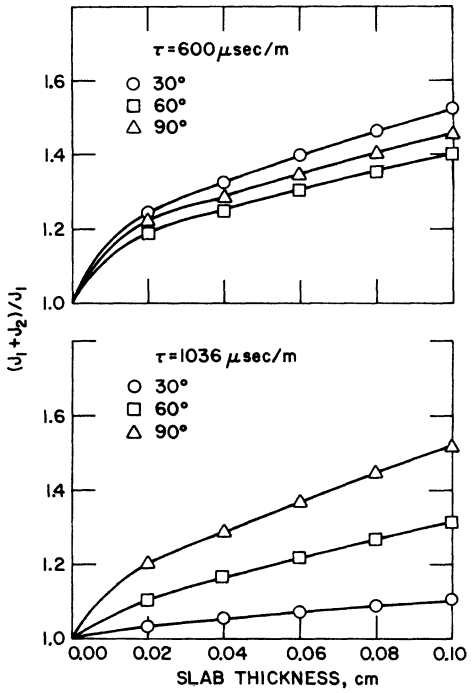

FIG. 4. $(J_1+J_2)/J_1$ vs gaseous-methane sample thickness for two scattered neutron energies with incident neutron energy 1036 μsec/m.

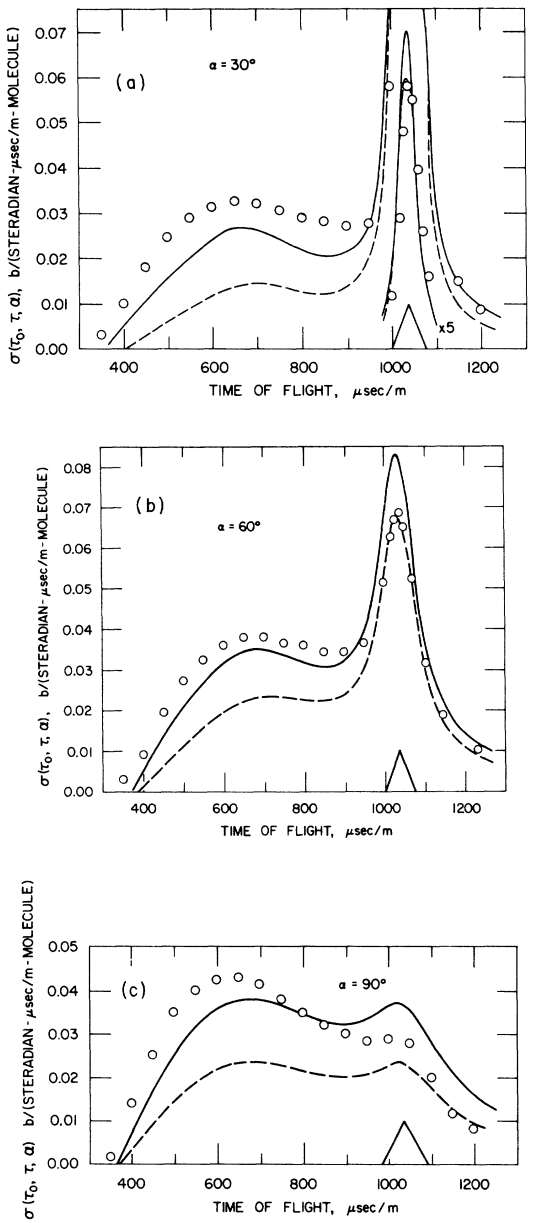

FIG. 5. Comparison of once- (dashed curve) and twice- (solid curve) scattered cross sections with measurements for liquid methane at 98°K. The small triangle indicates the position and width of the incident spectrum.

absolute units with the cold-neutron measurements of Dasannacharya and Venkataraman[8] for liquid methane (0.1 cm thick, 0.466 g/cm^3) at 89°K. In these calculations we have used a previously discussed scattering-law model.[10] Analytical $\sigma(\tau_0, \tau, \alpha)$'s for once- and twice-scattered neutrons are evaluated from Eq. (40) except that the detector response function was assumed to be a δ function. Owing to the unavailability of the normalization constant for measurements, the experimental points were area normalized to the calculated area for twice-scattered intensities. The incident neutron spectrum is shown by triangles in these figures. Note that the agreement between calculated and measured values is considerably improved by incorporating the double-scattering correction. When the actual detector response function is used, as opposed to the assumed δ function, the quasi-elastic peak would be less sharp which would result in a better agreement with the measurements.

IV. DISCUSSION

There are two ways of accounting for the multiple-scattering effect.[4] In one, called the subtraction method, the multiple-scattering contributions are subtracted from the measurement. Model calculations of the double-differential scattering cross sections are then compared with the corrected data. A major difficulty of this approach is the lack of an exact description for the scattering law. In fact, it is this lack of knowledge which makes inelastic-neutron scattering studies so interesting. In the second method, called the factor method, the correction is evaluated for an assumed scattering-law model. Satisfactory or unsatisfactory agreement of the corrected analytical results with measurements is then directly attributed to the assumed scattering model. If the multiple-scattering correction were insensitive to the scattering description, either of the two methods would be equally suitable. Unfortunately, that is not the case, as discussed later; hence the factor method is rec-

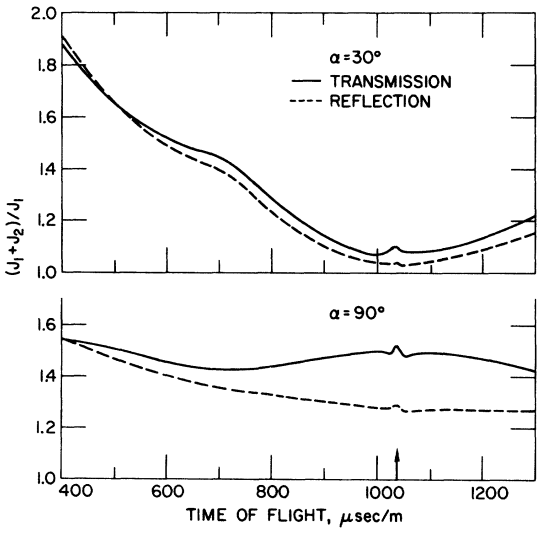

FIG. 6. $(J_1+J_2)/J_1$ vs time of flight in gaseous methane for transmission and reflection geometries. Sample thickness is 0.10 cm.

TABLE I. Once- and twice-scattered cross sections for liquid methane at 98 °K for two molecular-dynamics models.

τ	$\sigma_1(\tau_0, \tau, \alpha)$ [b/sr (μsec/m) molecule]		$\sigma(\tau_0, \tau, \alpha)$		$\frac{\sigma(\tau_0, \tau, \alpha)}{\sigma_1(\tau_0, \tau, \alpha)}$	
μsec/m	model A	model B	model A	model B	model A	model B
400	0.0003	0.0013	0.0045	0.0055	17.88	4.10
500	0.0061	0.0050	0.0162	0.0142	2.66	2.83
600	0.0120	0.0101	0.0244	0.0217	2.03	2.14
700	0.0136	0.0130	0.0249	0.0242	1.84	1.86
800	0.0128	0.0136	0.0221	0.0232	1.73	1.70
900	0.0139	0.0132	0.0218	0.0212	1.57	1.61
1000	0.0610	0.0608	0.0711	0.0711	1.16	1.17
1036	0.5285	0.5395	0.7482	0.7598	1.42	1.41
1050	0.2184	0.2217	0.2328	0.2366	1.07	1.07
1100	0.0209	0.0202	0.0270	0.0265	1.30	1.31
1200	0.0050	0.0046	0.0085	0.0082	1.70	1.77
1300	0.0025	0.0024	0.0048	0.0048	1.96	2.01

ommended.

We have presented the factor method for evaluating the double-scattering correction for inelastic-neutron scattering experiments for an infinite plane-slab specimen. The computer code DBLSCAT developed for such a study is written for an arbitrary scattering law. Although experiments are usually performed for transmission-type experiments, reflection geometries are also considered.

The detailed results for the double-scattering correction were presented in Sec. III. It was seen that the correction is extremely important in the inelastic region for small scattering angles (even for very thin samples). For example, in the case of 0.02-cm-thick highly compressed methane gas ($\Sigma t = 0.0912$), the correction is about 45% at 400 μsec/m for a scattering angle of 30°. For larger scattering angles (~90°), the correction is about 20–25% for all scattered-neutron energies. A small peak in the correction is attributed to the predominantly quasi-elastic peak in the scattering law.

The multiple-scattering correction is expected to depend on the scattering law. Since third- and higher-order scattering corrections are second-order effects, we have substantiated the above conjecture by evaluating the double-scattering correction using two different scattering models. Table I lists our results for once- and twice-scattered cross sections along with the fractional correction for the liquid-methane sample described earlier for a scattering angle of 30° with a monoenergetic neutron beam (1036 μsec/m). Model A is the one used in our compairson with the liquid-methane experiment, whereas model B is for Langevin-type translational and rotational description [see Eqs. (33)–(36)]. Note that the difference in correction is appreciable in the region in which scattering law itself differs appreciably. It is therefore concluded that the second-order correction is significantly sensitive to the scattering-law model.

Inelastic-neutron-scattering experiments using a plane-slab specimen can be done either in transmission or reflection geometries. Apart from the experimental details and their associated problems, it is desirable to know the effect of geometry on multiple-scattering correction. Figure 6 shows the second-order scattering correction as a function of the time of flight for both arrangements, assuming the same physical thickness (0.10 cm) and a highly compressed methane gas. Although the results for two cases are very close to each other for small scattering angles, the reflection geometry is distinctively preferable for large scattering angles. In addition, we find that the scattered-neutron currents for the reflection case are usually larger than the corresponding quantities for the transmission case.

We now briefly consider the third- and higher-order scattering events. Evaluation of the associated correction is prohibitively tedious and time consuming; hence approximate methods are generally employed. A common approximation for elastic scattering is suggested by Vineyard.[1] If the sample thickness is much less than one mean free path and the twice-scattered component has a roughly isotropic distribution, then it is assumed that

$$J_{n+1}/J_n = J_2/\bar{J}_1, \quad n = 2, 3, 4, \ldots \tag{41}$$

where $\bar{J}_1$ is the directionally averaged value of J_1. The multiple-scattering correction, defined by the quantity in brackets in Eq. (39), is given by

$$1 + \frac{J_2/J_1}{1 - J_2/\bar{J}_1} . \tag{42}$$

Even for the thickest sample considered in Sec. III, J_2/J_1 is less than 20%; hence, using the above equation the total multiple-scattering correction is estimated to be less than 25%.

In the case of inelastic scattering, Cocking[5] has

evaluated the intensity of a higher order of scattering by ignoring any further energy changes after the second scattering. An alternative method is the use of MUSE code. The detailed calculations of Slaggie[4] have shown that the third- and higher-order scattering corrections are less than 20% of the second-order scattering correction. It therefore appears that for most of the inelastic-scattering experiments the effect of third- and higher-order scattering corrections can be ignored, considering the current state of knowledge of the scattering model.

ACKNOWLEDGMENTS

The author would like to thank K. E. Larsson and S. Yip for some illuminating discussions.

*Work performed under the auspices of the U. S. Atomic Energy Commission.

[1]G. H. Vineyard, Phys. Rev. 96, 93 (1954).
[2]I. A. Blech and B. L. Averbach, Phys. Rev. 137, A1113 (1965).
[3]S. J. Cocking and C. R. T. Heard, Atomic Energy Research Establishment, Harwell, Berkshire, Report No. AERE-R5016, 1965 (unpublished).
[4]E. L. Slaggie, Nucl. Sci. Eng. 30, 199 (1967).
[5]S. J. Cocking, Atomic Energy Research Establishment, Harwell, Berkshire, Report No. AERE-R5867, 1968 (unpublished); K. R. Rao, B. A. Dasannacharya, and S. Yip (private communication).
[6]A. K. Agrawal, S. G. Das, and F. M. Mueller, Argonne National Laboratory Report No. ANL-7780, 1971 (unpublished).
[7]K. E. Larsson (private communication).
[8]B. A. Dasannacharya and G. Venkataraman, Phys. Rev. 156, 196 (1967).
[9]We use $\hbar = k_B = 1$.
[10]A. K. Agrawal and S. Yip, Nucl. Sci. Eng. 37, 369 (1969).
[11]A. K. Agrawal and S. G. Das, Trans. Am. Nucl. Soc. 14, 351 (1971).

PHYSICAL REVIEW A VOLUME 4, NUMBER 4 OCTOBER 1971

Bounds on the Thermodynamic Behavior of Systems with Generalized Coulomb Interactions

G. Stell*
Department of Mechanics, State University of New York, Stony Brook, New York 11790

and

O. Penrose†‡
Belfer Graduate School of Science, Yeshiva University, New York, New York 10033

(Received 1 December 1970)

Various lower and upper bounds are derived for the energy, free energy, and pressure of particles interacting via an r^{-n} pair potential in ν dimensions. The results include (i) lower bounds for mixtures with $n<2$, of the form const$\rho^{1+2/\nu}$ as ρ increases either isentropically or isothermally, complementing an upper bound of the same form in the isentropic case, recently derived by Kleban and Puff, and (ii) upper and lower bounds for the case $n>\nu$, $n>2$, which for the pressure are both of the form const$\rho^{1+n/\nu}$ as ρ increases isentropically.

We derive various upper and lower bounds for the energy, free energy, and pressure of a system of σ species of particles (including the $\sigma=1$ case) such that the interaction potential for a pair of particles of species i and j is $e_i e_j / r^n$, where r is their separation and n is a positive constant.

For $n<2$, our lower bounds are complementary to the recently derived upper bounds of Kleban and Puff,[1] and when combined with their bounds, show that the pressure p behaves under isentropic compression like $\rho^{1+2/\nu}$ for $n<2$ and like $\rho^{1+n/\nu}$ for $n>2$, $n>\nu$, where ρ is the density and ν the dimensionality. The case $n=1$, $\nu=3$ describes "real" matter (which we shall treat nonrelativistically) and is thus of special interest. In particular, our large-ρ results in this case are relevant to stellar matter. To ensure the existence of thermodynamic functions,[2] a charge-neutrality condition, $\sum_i e_i \rho_i = 0$, must be assumed[3] in the $n=1, \nu=3$ case (and perhaps for all $n<\nu$, although existence proofs are currently lacking except for $n=1, \nu=3$), where ρ_i is the density of the ith species; $\sum \rho_i = \rho$. For $n>\nu$, on the other hand, one expects the existence of thermodynamic functions if $e_i \geq 0$ for all i.

Our starting point is a form of the virial theorem[4]

$$\frac{p}{\rho} = \frac{2}{\nu} u_{\text{kin}} + \frac{n}{\nu} (u - u_{\text{kin}}) , \tag{1}$$